

Alteraxial Phonons in Collinear Magnets

Fuyi Wang^{1,†}, Junqi Xu^{1,†}, Xinqi Liu¹, Huaiqiang Wang^{2,*}, Lifa Zhang² and Haijun Zhang^{1,3,4,5,*}

¹ National Laboratory of Solid State Microstructures,

School of Physics, Nanjing University, Nanjing 210093, China

² Center for Quantum Transport and Thermal Energy Science,

Institute of Physics Frontiers and Interdisciplinary Sciences,

School of Physics and Technology, Nanjing Normal University, Nanjing 210023, China

³ Collaborative Innovation Center of Advanced Microstructures, Nanjing University, Nanjing 210093, China

⁴ Jiangsu Physical Science Research Center, Nanjing 210093, China

⁵ Jiangsu Key Laboratory of Quantum Information Science and Technology, Nanjing University, China*

(Dated: December 9, 2025)

Circularly polarized or axial phonons possessing nonzero angular momentum have attracted considerable interest. These phonons have finite magnetic moment and can couple to internal magnetic order. The rich magnetic structures enable phonon angular momentum (PAM) to acquire momentum-space textures analogous to electronic spin structures. However, a systematic framework for classifying these textures, especially their potential higher-order multipolar patterns, has remained elusive. Here, by employing magnetic point group analysis, we develop a complete classification of long-wavelength phonons in collinear magnets. Our theory distinguishes four fundamental types, including three families of magneto-axial phonons differentiated by symmetry and the parity (odd or even) of the PAM wave pattern. Strikingly, we reveal a full sequence of axial phonons exhibiting higher-order-wave (from p - to j -wave) PAM patterns covering both odd and even parities, which we term magneto-alteraxial phonons. Our high-throughput calculations predict hundreds of magnetic candidates hosting such magneto-alteraxial phonons. We have also performed *ab initio* calculations on representative materials to validate the proposed magneto-alteraxial phonon spectra and PAM patterns. Our work establishes a symmetry-guided design principle for axial phonons and related phenomena in magnetic materials.

Introduction. Circularly polarized phonons with finite angular momentum [1–3], recently termed axial phonons [4], have attracted growing research interest over the past decade [5–21]. Intriguingly, nonzero phonon angular momentum (PAM) can yield an effective phonon magnetic moment [13, 22–27], which enables the coupling of axial phonons to both external magnetic fields and internal magnetic moments [8, 28–36]. Such couplings have been shown to give rise to various phono-magnetic effect, including the phonon Zeeman effect [37, 38], the ultrafast Einstein-de Haas effect [32, 39] and the phonon Barnett effect [22, 31]. Specifically, the phonon Zeeman effect can induce observable frequency splittings between left- and right-circularly polarized phonons in magnetic materials, as demonstrated in $\text{Co}_3\text{Sn}_2\text{S}_2$ [40–42]. Despite recent progress, the interplay between axial phonons and magnetic order still remains largely unexplored.

A key open question regarding axial phonons in magnetic materials is how crystal and magnetic structures shape momentum-space phonon Zeeman splittings and resultant PAM patterns. Analogous to the classification of collinear magnets (ferro-, antiferro-, alter-magnets) by their magnetic structures [44–46], phonons in collinear magnets can, in principle, be similarly categorized into such distinct types, as schematized in Fig. 1. Ferro-type axial phonons [Fig. 1(a)] are characterized by circular lattice vibrations of a single handedness in real space and circularly polarized phonon spectra in momentum space. Antiferro-type nonaxial phonons [Fig. 1(b)] feature \mathcal{PT} -symmetric circular vibrations in real space and unpolar-

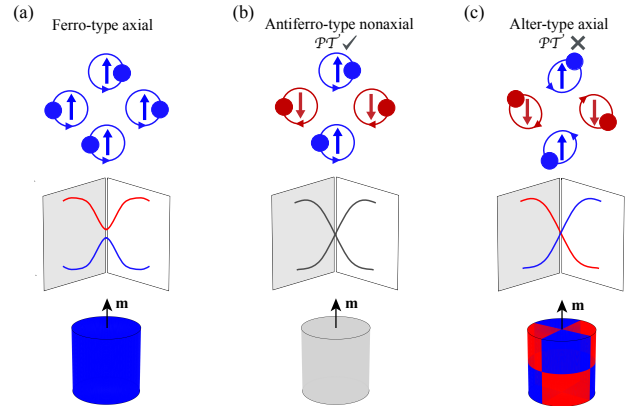


FIG. 1. Schematics of three distinct types of circularly polarized phonons in collinear magnets. Circular lattice vibrations in real space (top row), long-wavelength phonon spectra (middle row) and angular momentum patterns in momentum space (bottom row) for (a) ferro-type axial, (b) antiferro-type nonaxial and (c) alter-type axial phonons in collinear magnets, respectively. The magnetization direction is set as the quantization axis for the phonon angular momentum.

ized phonon spectra with vanishing PAM in momentum space. Alter-type axial phonons [Fig. 1(c)] exhibit real-space alternating circular vibrations that are not connected by \mathcal{PT} symmetry and alternating circularly polarized phonon spectra with wave-modulated PAM patterns in momentum space. However, a comprehensive group-theoretical study of phonons in collinear magnets is still

TABLE I. Complete classification of phonons in collinear magnets. Phonons are categorized into four types by magnetic point group symmetry, with distinct phonon angular momentum (PAM) wave patterns: nonaxial, centrosymmetric-even-wave (s -, d -, g -, i -wave), noncentrosymmetric-odd-wave (p -, f -, h -, j -wave), and noncentrosymmetric-even-wave (s -, d -, g -, i -wave). The s -wave pattern describes ferromagneto-axial phonons, whereas higher-order patterns (p - to j -wave) correspond to magneto-alteraxial phonons. Magnetic point groups are given in the UNI notation [43]. Parentheses are used to specify the orientation of the magnetic axis.

Type	Wave	Magnetic Point Group
Non-axial	N/A	$6/mmm.1'$, $6'/mmm'$, $6/m'm'm'$, $m'm'm'$, $6/m.1'$, $6'/m$, $6/m'mm$, $6/m'$, $4/m'mm$, $4/m'm'm'$, $4'/m'm'm$, $4/m'$, $4/mmm.1'$, $4/m.1'$, $4'/m'$, $2'/m$, $2/m'$, $2/m.1'$, $m'mm$, $mmm.1'$, $\bar{1}$, $\bar{1}.1'$, $\bar{3}m$, $\bar{3}m'$, $\bar{3}m.1'$, $\bar{3}.1'$, $\bar{3}$
Centro-even	s -wave	$6/m.1$, $m'm'm(z)$, $2/m.1(y)$, $4/mm'm'$, $\bar{3}m'$, $4/m.1$, $\bar{3}.1$, $\bar{1}.1$, $2'/m'(xz)$, $6/mm'm'$
	d -wave	$2'/m'(y)$, $m'm'm(y)$, $mmm.1$, $2/m.1(xz)$, $mmm.1$, $m'm'm(x)$, $mmm.1$, $4'/m$, $4'/mm'm$
	g -wave	$4/mmm.1$, $\bar{3}m.1$, $6'/m'mm'$, $6'/m'$
	i -wave	$6/mmm.1$
Noncentro-odd	p -wave	$6.1'$, $m.1'$, $2.1'$, $4'$, $222.1'$, $6'22'$, $622.1'$, $422.1'$, 32.1 , 622.1 , 222.1 , $32.1'$, $2.1(xz)$, $4'22'$, $6'$, $3.1'$, 422.1 , $m'(y)$, $4.1'$, $1.1'$, $mm2.1(x)$, $m'm'2(x)$, 222.1 , $222.1'$, $m'm'2(x)$, $m.1(xz)$, $m.1'$, $mm2.1'(x)$, $2.1'$, $2'(y)$, $2'2'2(y)$, $m'm'2(y)$, 222.1 , $222.1'$, $mm2.1'(y)$, $2'2'2(x)$, $mm2.1(y)$
	f -wave	$\bar{4}.1'$, $mm2.1'(z)$, $\bar{4}2m.1$, $\bar{4}2m.1'$, $3m.1$, $\bar{6}m2.1'$, $\bar{6}'m2'$, $3m.1'$, $\bar{6}'m'2$, $\bar{6}m2.1$, $\bar{6}'$, $\bar{6}.1'$
	h -wave	$4mm.1'$
	j -wave	$6mm.1'$
Noncentro-even	s -wave	$m'm'2'(y)$, $2'2'2(z)$, $62'2'$, $2'(xz)$, 1.1 , 6.1 , $m'm'2(z)$, $2.1(y)$, $\bar{4}2'm'$, 3.1 , $\bar{4}.1$, $32'$, $4m'm'$, $m'(xz)$, $\bar{6}m'2'$, $6m'm'$, $m.1(y)$, $42'2'$, 4.1 , $3m'$, $\bar{6}.1$
	d -wave	$\bar{4}'$, $mm2.1(z)$, $\bar{4}'2m'$, $m'm'2'(z)$, $\bar{4}'2'm$, $4'm'm$
	g -wave	$4mm.1$, $6'mm'$
	i -wave	$6mm.1$

lacking, thereby significantly hindering the identification of magnetic materials hosting alter-type phonons.

In this work, based on magnetic point group (MPG) analysis, we perform a complete group-theoretical classification of long-wavelength phonons in collinear magnets. Specifically, we divide them into four categories distinguished by symmetry and momentum-space PAM wave patterns: one nonaxial type and three magnetoaxial types, comprising centrosymmetric even-wave, noncentrosymmetric odd-wave, and noncentrosymmetric even-wave phonons. Remarkably, beyond the ferromagneto-axial (s -wave) phonon, we reveal higher-order-wave PAM patterns featuring one to seven nodal surfaces of vanishing PAM crossing the Γ point. These correspond to the complete series from p - to j -wave magneto-alteraxial phonons, encompassing both odd- and even-parity wave patterns [see Supplemental Material (SM) [47]]. We have also performed high-throughput calculations of magnetic materials, and predicted hundreds of candidates hosting magneto-alteraxial phonons. We further present *ab initio* calculations of the magnetic phonon spectra and PAM patterns for three representative magneto-alteraxial phonon materials spanning distinct categories, namely, CrSb, Cr₂SbAs, and MnSe. By establishing a systematic framework for axial phonons in collinear magnets, our work opens the door to the discovery and study of magneto-alteraxial phonons.

Symmetry-based classification scheme. The concept of magneto-axial phonons is based on the magnitude of the PAM defined with the collinear magnetization direction (labeled as \vec{e}_m direction) as the quantization axis. For a single phonon mode $\epsilon_{\mathbf{q}}$ with \mathbf{q} denoting its wavevector, this magnitude corresponds to the phonon circular polarization along \vec{e}_m direction, which is given by

$$j_m(\mathbf{q}) = \langle \epsilon_{\mathbf{q}} | (|\mathbf{R}_m\rangle\langle\mathbf{R}_m| - |\mathbf{L}_m\rangle\langle\mathbf{L}_m|) | \epsilon_{\mathbf{q}} \rangle \hbar. \quad (1)$$

Here, $|\epsilon_{\mathbf{q}}\rangle$ denotes the phonon-mode eigenvector, \hbar is the Planck's constant, and $|\mathbf{R}_m\rangle$ ($|\mathbf{L}_m\rangle$) represents the right-handed (left-handed) circularly polarized eigenstate with angular momentum \hbar ($-\hbar$) along \vec{e}_m direction. A phonon mode is termed magnetoaxial when it possesses a nonzero $j_m(\mathbf{q})$.

Throughout this work, we consider long-wavelength phonon modes near the Γ point in collinear magnets, whose symmetry properties are characterized by a MPG denoted as G [43]. Under a symmetry operation $\mathcal{G} \in G$, the angular momentum $j_m(\mathbf{q})$ satisfies

$$j_m(\mathcal{G}\mathbf{q}) = \eta(\mathcal{T})\chi(\mathcal{R})j_m(\mathbf{q}). \quad (2)$$

Here, \mathcal{T} is the time-reversal operation, and $\eta(\mathcal{T}) = -1$ ($+1$) when \mathcal{T} operation is (not) contained in \mathcal{G} . \mathcal{R} denotes the point-group part operation in \mathcal{G} , and $\chi(\mathcal{R}) = +1$ (-1) if \mathcal{R} preserves (switches) the handedness of the circularly polarized states $|\mathbf{R}_m\rangle$ and $|\mathbf{L}_m\rangle$. Specifically, time-reversal symmetry \mathcal{T} yields $j_m(-\mathbf{q}) = -j_m(\mathbf{q})$,

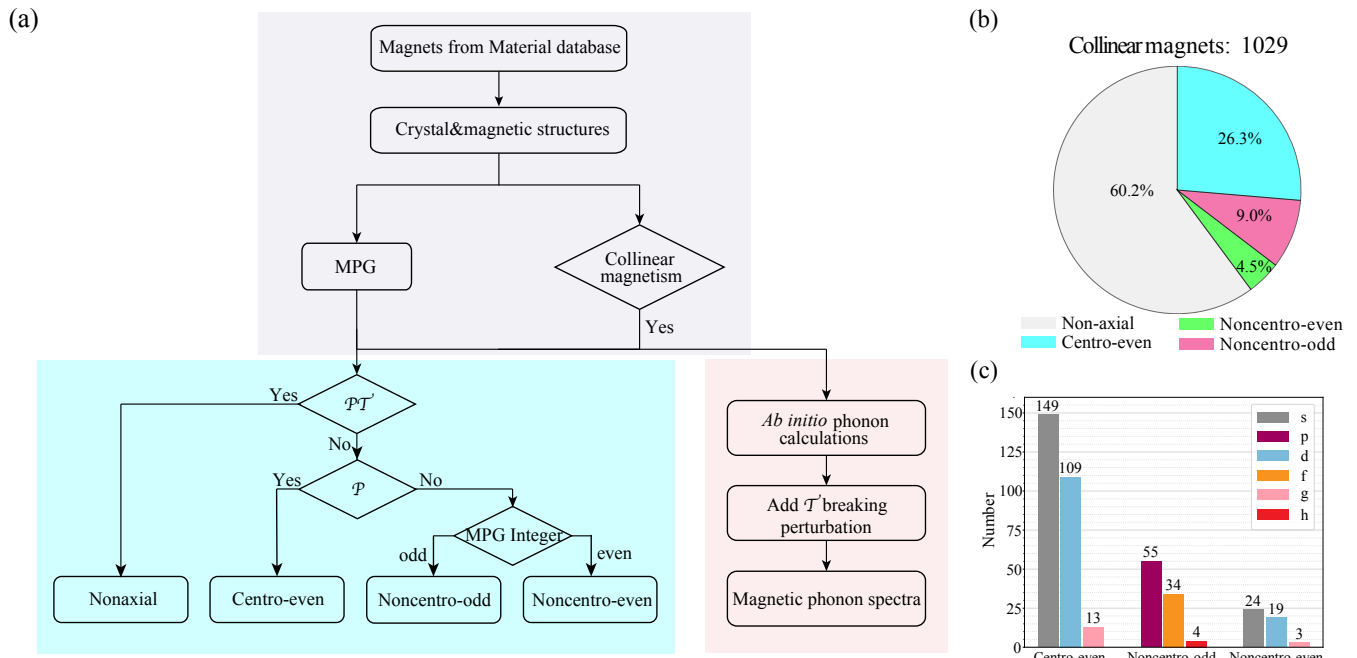


FIG. 2. High-throughput phonon calculations in collinear magnets. The workflow (a) consists of three parts: The gray-shaded part filters out collinear magnets from material databases and provides their crystal and magnetic structures along with the corresponding magnetic point groups (MPG); The cyan-shaded part classifies the phonon type according to the MPG, where the MPG integer denotes the number of symmetry-enforced nodal surfaces of vanishing phonon angular momentum crossing the Γ point; The pink-shaded part performs *ab initio* calculations of magnetic phonon spectra. (b, c) High-throughput screening for all 1029 collinear magnets from the MAGNDATA database, with (b) distribution of materials across the four distinct phonon types and (c) number of materials hosting different wave patterns within the three magneto-axial phonon families.

while inversion symmetry \mathcal{P} gives $j_m(-\mathbf{q}) = j_m(\mathbf{q})$. Consequently, in the presence of the combined \mathcal{PT} symmetry, $j_m(\mathbf{q}) = 0$ is always satisfied, and the corresponding phonons are nonaxial.

Breaking the combined \mathcal{PT} symmetry in collinear magnets enables a nonzero $j_m(\mathbf{q})$, thereby leading to the emergence of magnetoaxial phonon modes. Interestingly, if at least one symmetry operation yields $\eta(\mathcal{T})\chi(\mathcal{R}) = -1$, then j_m vanishes at the Γ point, while alternating in sign across the surrounding Brillouin zone (BZ). This results in nodal surfaces of vanishing $j_m(\mathbf{q})$ which pass through the Γ point in the three-dimensional BZ. The number of such nodal surfaces, determined from MPG constraints in Eq. (2), ranges from 1 to 7, corresponding to *p*-, *d*-, *f*-, *g*-, *h*-, *i*-, *j*-wave magnetoalteraxial phonons, respectively (see the SM for detailed illustrations). In contrast, if no symmetry operations gives $\eta(\mathcal{T})\chi(\mathcal{R}) = -1$, then no such symmetry-enforced nodal surfaces exist, and $j_m(\mathbf{q})$ generically exhibits *s*-wave feature in the BZ, thereby termed ferromagnetoaxial phonons.

Based on the above symmetry analysis, we categorize long-wavelength phonons in collinear magnets into four distinct types according to the underlying symmetry and the wave parity of the PAM pattern: (i) \mathcal{PT} -symmetric nonaxial phonons; (ii) Centrosymmetric-

even-wave (*s*-, *d*-, *g*-, *i*-wave) magnetoaxial phonons; (iii) Noncentrosymmetric-odd-wave (*p*-, *f*-, *h*-, *j*-wave) magnetoaxial phonons; (iv) Noncentrosymmetric-even-wave (*s*-, *d*-, *g*-, *i*-wave) magnetoaxial phonons. The complete classification for all collinear MPGs is presented in Table I. Notably, since $j_m(\mathbf{q})$ is odd under time-reversal symmetry \mathcal{T} , the breaking of \mathcal{T} is a necessary condition for the emergence of both type (ii) and type (iv) phonons which feature even-wave PAM and are inherent to magnetic systems. In realistic magnetic materials, such \mathcal{T} -breaking terms typically arise from spin-phonon [30, 34, 38, 50, 51] or magnon-phonon couplings [52–60], which usually constitute perturbative contributions to the phonon Hamiltonian.

High-throughput calculations. To search for realistic materials hosting magnetoaxial phonons, we performed high-throughput phonon calculations on magnetic materials from databases such as MAGNDATA [61, 62] and Materials Project [63]. The calculation workflow, as depicted in Fig. 2(a), comprises two primary tasks after obtaining the crystal and magnetic structures, namely, determining the MPG-based phonon type and conducting *ab initio* calculations of magnetic phonon spectra. It is worth mentioning that our *ab initio* phonon calculations incorporate the Raman-type spin-phonon coupling inud-

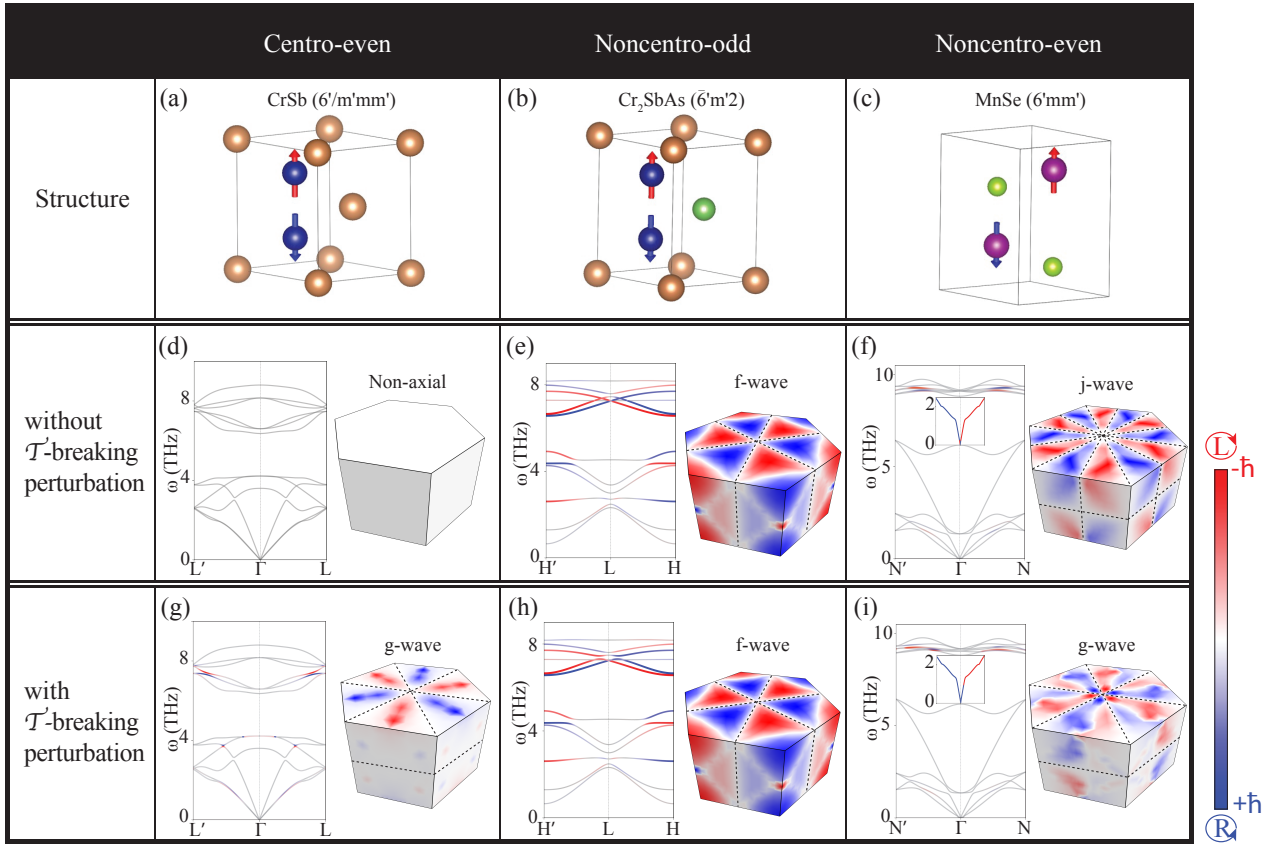


FIG. 3. Phonon spectra and phonon angular momentum (PAM) patterns from *ab initio* calculations on representative materials hosting three different types of magneto-alteraxial phonons. CrSb (centrosymmetric-even-wave), Cr₂SbAs (noncentrosymmetric-odd-wave), and MnSe (noncentrosymmetric-even-wave) are selected as illustrative cases. For each material, the top row shows the crystal and magnetic structures, the middle (bottom) row presents the \mathcal{T} -symmetric (\mathcal{T} -broken) phonon spectra and PAM patterns near the Γ point in the absence (presence) of \mathcal{T} -breaking perturbations.

ced from electron-phonon interaction as the \mathcal{T} -breaking perturbation [64], as implemented via a recently developed method by some of the authors [38] (see the SM for details).

Figures 2(b) and 2(c) summarized our results for all 1029 collinear magnets from the MAGNDATA database [see Supplemental Material [47] for the results of Material Project database]. Of these 1,029 materials, 619 (60.2%) host nonaxial phonons. The remaining 410 materials host magnetoaxial phonons, distributed as follows: 271 (26.3%) are centrosymmetric even-wave, 93 (9.0%) are noncentrosymmetric odd-wave, and 46 (4.5%) are noncentrosymmetric even-wave. Notably, we uncover 237 magnets that host magneto-alteraxial phonons containing both odd- and even-parity wave patterns, in addition to 173 materials exhibiting nodeless *s*-wave magnetoaxial phonons.

Representative materials. Our calculations reveal that magneto-alteraxial phonons featuring higher-order PAM wave patterns exist in materials across

all magnetic types, including ferromagnets, antiferromagnets, and altermagnets. Inspired by recent progresses in altermagnetism, we select three altermagnets as representative materials (see the SM for other magnets), each hosting a distinct type of magneto-alteraxial phonon: CrSb [45] (centrosymmetric-even-wave); Cr₂SbAs (noncentrosymmetric-odd-wave); and MnSe (noncentrosymmetric-even-wave), as detailed below.

CrSb exhibits an out-of-plane collinear magnetic order with antiparallel-aligned moments on Cr atoms [see Fig.3(a)], which belongs to the MPG $6'/m'mm'$. Within the spin-group description, it is classified as a *g*-wave altermagnet. It possesses inversion symmetry with Cr atoms acting as the inversion center. Consequently, in the absence of \mathcal{T} -breaking perturbation, the phonon spectrum of CrSb preserves the combined \mathcal{PT} symmetry, yielding nonaxial phonons with vanishing PAM [Fig. 3(d)]. Notably, when \mathcal{T} -breaking perturbation is incorporated, magneto-alteraxial phonons with even parity *g*-wave PAM pattern emerge. This is evidenced by

the phonon spectrum and PAM distribution [Fig. 3(g)] characterized by four nodal-surfaces with vanishing PAM crossing the Γ point (three vertical surfaces connected by C_{3z} and one horizontal $q_z = 0$ surface enforced by $C_{2z}\mathcal{T}$ symmetry).

Cr_2SbAs is obtained by substituting As for one Sb site from CrSb [see Fig. 3(b)], thereby breaking the inversion symmetry and lowering the MPG to $\bar{6}'m'2$. Without the \mathcal{T} -breaking perturbation, the phonon spectrum exhibits odd-parity f -wave PAM pattern, with three vertical zero-PAM nodal surfaces passing through the Γ point [Fig. 3(e)]. This f -wave pattern persists even when the \mathcal{T} -breaking perturbation is present, as shown in Fig. 3(h). In fact, the f -wave pattern results from the removal of the $q_z = 0$ nodal surface in CrSb due to the broken $C_{2z}\mathcal{T}$ symmetry. Interestingly, Cr_2SbAs remains a g -wave altermagnet, since its electronic structure is described by spin groups [65, 66] distinct from the MPG description of its phonon spectrum.

MnSe is a noncentrosymmetric magnet hosting out-of-plane antiparallel alignment of Mn moments [see Fig. 3(c)], described by the MPG $6'mm'$. As shown in Fig. 3(f), the unperturbed phonon spectrum of MnSe with preserved \mathcal{T} symmetry exhibits an odd-parity j -wave PAM pattern, featuring seven zero-PAM nodal surfaces crossing the Γ point: six vertical surfaces related by C_{6z} symmetry, and one horizontal surface ($q_z = 0$) enforced by $C_{2z}\mathcal{T}$ symmetry. Under a \mathcal{T} -breaking perturbation, the C_{6z} symmetry is reduced to $C_{6z}\mathcal{T}$, whereas $C_{2z}\mathcal{T}$ remains. This eliminates three vertical nodal surfaces, which in turn changes the PAM pattern from odd-parity j -wave to even parity g -wave. It is worth noting that all noncentrosymmetric even-wave PAM patterns can be derived from an unperturbed higher-order-wave odd-parity pattern that preserves \mathcal{T} symmetry, and the full derivation based on compatibility relations for each case is detailed in the SM.

Conclusion. We have established a comprehensive group-theoretical framework to systematically classify axial phonons in collinear magnets and uncovered a complete hierarchy of magneto-alteraxial phonons characterized by higher-order-wave momentum-space PAM patterns. Our high-throughput screening identifies numerous candidate materials and *ab initio* calculations are further performed on representative materials to confirm magneto-alteraxial phonons as well as their PAM patterns. Our work not only significantly enriches the family of axial phonons, but also opens a new avenue in phonon engineering via magneto-phononic effects.

Acknowledgments. This work is partly supported by National Key Projects for Research and Development of China (Grants No. 2024YFA1409100, No. 2021YFA1400400, No. 2022YFA1403602, and No. 2023YFA1407001), the Natural Science Foundation of Jiangsu Province (Grants No. BK20253012, No. BK20252117, No. BK20233001, No. BK20243011,

and No. BK20220032), the Natural Science Foundation of China (Grants No. 12534007, No. 92365203 and No.12174182) and the e-Science Center of Collaborative Innovation Center of Advanced Microstructures.

* zhanghj@nju.edu.cn; hqwang@nju.edu.cn

- [1] L. Zhang and Q. Niu, Angular Momentum of Phonons and the Einstein-de Haas Effect, *Phys. Rev. Lett.* **112**, 085503 (2014).
- [2] L. Zhang and Q. Niu, Chiral Phonons at High-Symmetry Points in Monolayer Hexagonal Lattices, *Phys. Rev. Lett.* **115**, 115502 (2015).
- [3] H. Zhu, J. Yi, M.-Y. Li, J. Xiao, L. Zhang, C.-W. Yang, R. A. Kaindl, L.-J. Li, Y. Wang, and X. Zhang, Observation of chiral phonons, *Science* **359**, 579 (2018).
- [4] D. M. Juraschek, R. M. Geilhufe, H. Zhu, M. Basini, P. Baum, A. Baydin, S. Chaudhary, M. Fechner, B. Flebus, G. Grissonnanche, A. I. Kirilyuk, M. Lemesko, S. F. Maehrlein, M. Mignolet, S. Murakami, Q. Niu, U. Nowak, C. P. Romao, H. Rostami, T. Satoh, N. A. Spaldin, H. Ueda, and L. Zhang, Chiral phonons, *Nat. Phys.* **21**, 1532 (2025).
- [5] X. Chen, X. Lu, S. Dubey, Q. Yao, S. Liu, X. Wang, Q. Xiong, L. Zhang, and A. Srivastava, Entanglement of single-photons and chiral phonons in atomically thin wse2, *Nat. Phys.* **15**, 221 (2019).
- [6] G. Grissonnanche, S. Thériault, A. Gourgout, M.-E. Boulanger, E. Lefrançois, A. Ataei, F. Laliberté, M. Dion, J.-S. Zhou, S. Pyon, *et al.*, Chiral phonons in the pseudogap phase of cuprates, *Nat. Phys.* **16**, 1108 (2020).
- [7] K. Ishito, H. Mao, Y. Kousaka, Y. Togawa, S. Iwasaki, T. Zhang, S. Murakami, J.-i. Kishine, and T. Satoh, Truly chiral phonons in α -HgS, *Nat. Phys.* **19**, 35 (2023).
- [8] N. Shabala and R. M. Geilhufe, Phonon Inverse Faraday Effect from Electron-Phonon Coupling, *Phys. Rev. Lett.* **133**, 266702 (2024).
- [9] T. Kahana, D. A. B. Lopez, and D. M. Juraschek, Light-induced magnetization from magnonic rectification, *Sci. Adv.* **10**, eado0722 (2024).
- [10] L. Klebl, A. Schobert, M. Eckstein, G. Sangiovanni, A. V. Balatsky, and T. O. Wehling, Ultrafast pseudomagnetic fields from electron-nuclear quantum geometry, *Phys. Rev. Lett.* **134**, 016705 (2025).
- [11] C. Paiva, M. Fechner, and D. M. Juraschek, Dynamically induced multiferroic polarization, *Phys. Rev. Lett.* **135**, 066702 (2025).
- [12] H. Ueda, M. García-Fernández, S. Agrestini, C. P. Romao, J. van den Brink, N. A. Spaldin, K.-J. Zhou, and U. Staub, Chiral phonons in quartz probed by X-rays, *Nature* **618**, 946 (2023).
- [13] F. G. G. Hernandez, A. Baydin, S. Chaudhary, F. Tay, I. Katayama, J. Takeda, H. Nojiri, A. K. Okazaki, P. H. O. Rappl, E. Abramof, M. Rodriguez-Vega, G. A. Fiete, and J. Kono, Chiral Phonons with Giant Magnetic Moments in a Topological Crystalline Insulator, *Sci. Adv.* **9**, eadj4074 (2023).
- [14] K. Kim, E. Vetter, L. Yan, C. Yang, Z. Wang, R. Sun, Y. Yang, A. H. Comstock, X. Li, J. Zhou, L. Zhang, W. You, D. Sun, and J. Liu, Chiral-phonon-activated spin Seebeck effect, *Nat. Mater.* **22**, 322 (2023).

- [15] K. Luo and X. Dai, Transverse peierls transition, *Phys. Rev. X* **13**, 011027 (2023).
- [16] F. G. Hernandez, A. Baydin, S. Chaudhary, F. Tay, I. Katayama, J. Takeda, H. Nojiri, A. K. Okazaki, P. H. Rappl, E. Abramof, *et al.*, Observation of interplay between phonon chirality and electronic band topology, *Sci. adv.* **9**, eadj4074 (2023).
- [17] S. Zhang, Z. Huang, M. Du, T. Ying, L. Du, and T. Zhang, The chirality of phonons: Definitions, symmetry constraints, and experimental observation, [arXiv:2503.22794](https://arxiv.org/abs/2503.22794) (2025).
- [18] C. P. Romao and D. M. Juraschek, Phonon-Induced Geometric Chirality, *ACS Nano* **18**, 29550 (2024).
- [19] Y. Yang, Z. Xiao, Y. Mao, Z. Li, Z. Wang, T. Deng, Y. Tang, Z.-D. Song, Y. Li, H. Yuan, M. Shi, and Y. Xu, Catalogue of chiral phonon materials, [arXiv:2506.13721](https://arxiv.org/abs/2506.13721) (2025).
- [20] Y. Chen, W. Qin, S. Zhang, P. Cui, Q. Niu, and Z. Zhang, Emergence of chiral phonons in two-dimensional kagome lattices harboring electronic chirality, *Phys. Rev. Lett.* **135**, 126608 (2025).
- [21] D. Yao and S. Murakami, Theory of spin magnetization driven by chiral phonons, *Phys. Rev. B* **111**, 134414 (2025).
- [22] J. Luo, T. Lin, J. Zhang, X. Chen, E. R. Blackert, R. Xu, B. I. Yakobson, and H. Zhu, Large effective magnetic fields from chiral phonons in rare-earth halides, *Science* **382**, 698 (2023).
- [23] Y. Ren, C. Xiao, D. Saporov, and Q. Niu, Phonon Magnetic Moment from Electronic Topological Magnetization, *Phys. Rev. Lett.* **127**, 186403 (2021).
- [24] X.-W. Zhang, Y. Ren, C. Wang, T. Cao, and D. Xiao, Gate-Tunable Phonon Magnetic Moment in Bilayer Graphene, *Phys. Rev. Lett.* **130**, 226302 (2023).
- [25] C. Tang, G. Ye, C. Nnokwe, M. Fang, L. Xiang, M. Mahjour-Samani, D. Smirnov, E.-H. Yang, T. Wang, L. Zhang, R. He, and W. Jin, Exciton-activated effective phonon magnetic moment in monolayer MoS_2 , *Phys. Rev. B* **109**, 155426 (2024).
- [26] H. Mustafa, C. Nnokwe, G. Ye, M. Fang, S. Chaudhary, J.-A. Yan, K. Wu, C. J. Cunningham, C. M. Hemesath, A. J. Stollenwerk, P. M. Shand, E.-H. Yang, G. A. Fiete, R. He, and W. Jin, Origin of Large Effective Phonon Magnetic Moments in Monolayer MoS_2 , *ACS Nano* **19**, 11241 (2025).
- [27] R. Xue, Z. Qiao, Y. Gao, and Q. Niu, Extrinsic mechanisms of phonon magnetic moment, *Phys. Rev. Lett.* **135**, 106605 (2025).
- [28] S. Park and B.-J. Yang, Phonon Angular Momentum Hall Effect, *Nano Lett.* **20**, 7694 (2020).
- [29] T. Yin, K. A. Ulman, S. Liu, A. Granados del Águila, Y. Huang, L. Zhang, M. Serra, D. Sedmidubsky, Z. Sofer, S. Y. Quek, *et al.*, Chiral phonons and giant magneto-optical effect in CrBr_3 2d magnet, *Adv. Mater.* **33**, 2101618 (2021).
- [30] J. Bonini, S. Ren, D. Vanderbilt, M. Stengel, C. E. Dreyer, and S. Coh, Frequency Splitting of Chiral Phonons from Broken Time-Reversal Symmetry in CrI_3 , *Phys. Rev. Lett.* **130**, 086701 (2023).
- [31] C. S. Davies, F. G. N. Fennema, A. Tsukamoto, I. Razdolski, A. V. Kimel, and A. Kirilyuk, Phononic switching of magnetization by the ultrafast Barnett effect, *Nature* **628**, 540 (2024).
- [32] S. R. Tauchert, M. Volkov, D. Ehberger, D. Kazenwadel, M. Evers, H. Lange, A. Donges, A. Book, W. Kreuzpaintner, U. Nowak, and P. Baum, Polarized phonons carry angular momentum in ultrafast demagnetization, *Nature* **602**, 73 (2022).
- [33] D. Lujan, J. Choe, S. Chaudhary, G. Ye, C. Nnokwe, M. Rodriguez-Vega, J. He, F. Y. Gao, T. N. Nunley, E. Baldini, J. Zhou, G. A. Fiete, R. He, and X. Li, Spin-orbit exciton-induced phonon chirality in a quantum magnet, *Proc. Natl. Acad. Sci. USA* **121**, e2304360121 (2024).
- [34] S. Ren, J. Bonini, M. Stengel, C. E. Dreyer, and D. Vanderbilt, Adiabatic Dynamics of Coupled Spins and Phonons in Magnetic Insulators, *Phys. Rev. X* **14**, 011041 (2024).
- [35] J. Okamoto, C. Y. Mou, H. Y. Huang, G. Channagowdra, C. Won, K. Du, X. Fang, E. V. Komleva, C. T. Chen, S. V. Streltsov, A. Fujimori, S.-W. Cheong, and D. J. Huang, Altermagnetic boosting of chiral phonons, [arXiv:2512.00388](https://arxiv.org/abs/2512.00388) [10.48550/arXiv.2512.00388](https://doi.org/10.48550/arXiv.2512.00388) (2025).
- [36] N. Shabala, F. Tietjen, and R. M. Geilhufe, Axial phonomagnetic effects, [arXiv:2511.03329](https://arxiv.org/abs/2511.03329) (2025).
- [37] D. M. Juraschek, T. Neuman, and P. Narang, Giant effective magnetic fields from optically driven chiral phonons in $4f$ paramagnets, *Phys. Rev. Res.* **4**, 013129 (2022).
- [38] F. Wang, X. Liu, H. Sun, H. Wang, S. Murakami, L. Zhang, H. Zhang, and D. Xing, Ab initio theory of phonon magnetic moments induced by electron-phonon coupling in magnetic materials, [arXiv:2503.10160](https://arxiv.org/abs/2503.10160) (2025).
- [39] C. Dornes, Y. Acremann, M. Savoini, M. Kubli, M. J. Neugebauer, E. Abreu, L. Huber, G. Lantz, C. a. F. Vaz, H. Lemke, E. M. Bothschafter, M. Porer, V. Esposito, L. Rettig, M. Buzzi, A. Alberca, Y. W. Windsor, P. Beaud, U. Staub, D. Zhu, S. Song, J. M. Glowina, and S. L. Johnson, The ultrafast Einstein-de Haas effect, *Nature* **565**, 209 (2019).
- [40] M. Che, J. Liang, Y. Cui, H. Li, B. Lu, W. Sang, X. Li, X. Dong, L. Zhao, S. Zhang, T. Sun, W. Jiang, E. Liu, F. Jin, T. Zhang, and L. Yang, Magnetic order induced chiral phonons in a ferromagnetic weyl semimetal, *Phys. Rev. Lett.* **134**, 196906 (2025).
- [41] R. Yang, Y.-Y. Zhu, M. Steigleder, Y.-C. Liu, C.-C. Liu, X.-G. Qiu, T. Zhang, and M. Dressel, Inherent circular dichroism of phonons in magnetic weyl semimetal $\text{Co}_3\text{Sn}_2\text{S}_2$, *Phys. Rev. Lett.* **134**, 196905 (2025).
- [42] S. Zhang, M. Wang, and T. Zhang, General ab initio framework for chiral phonons induced by electronic order, [arXiv:2509.09253](https://arxiv.org/abs/2509.09253) (2025).
- [43] B. J. Campbell, H. T. Stokes, J. M. Perez-Mato, and J. Rodríguez-Carvajal, Introducing a unified magnetic space-group symbol, *Found. Crystallogr.* **78**, 99 (2022).
- [44] L. Šmejkal, Emerging Research Landscape of Altermagnetism, *Phys. Rev. X* **12** (2022).
- [45] L. Šmejkal, Beyond Conventional Ferromagnetism and Antiferromagnetism: A Phase with Nonrelativistic Spin and Crystal Rotation Symmetry, *Phys. Rev. X* **12** (2022).
- [46] C. Song, H. Bai, Z. Zhou, L. Han, H. Reichlova, J. H. Dil, J. Liu, X. Chen, and F. Pan, Altermagnets as a new class of functional materials, *Nat. Rev. Mater.* **10**, 473 (2025).
- [47] See the Supplemental Material, which includes Refs. [48, 49], for additional information about the methods and additional data and discussion.

- [48] P. Giannozzi, S. Baroni, N. Bonini, M. Calandra, R. Car, C. Cavazzoni, D. Ceresoli, G. L. Chiarotti, M. Cococcioni, I. Dabo, A. Dal Corso, S. De Gironcoli, S. Fabris, G. Fratesi, R. Gebauer, U. Gerstmann, C. Gougoussis, A. Kokalj, M. Lazzeri, L. Martin-Samos, N. Marzari, F. Mauri, R. Mazzarello, S. Paolini, A. Pasquarello, L. Paulatto, C. Sbraccia, S. Scandolo, G. Sclauzero, A. P. Seitsonen, A. Smogunov, P. Umari, and R. M. Wentzcovitch, QUANTUM ESPRESSO: A modular and open-source software project for quantum simulations of materials, *J. Phys.: Condens. Matter* **21**, 395502 (2009).
- [49] P. Giannozzi, O. Andreussi, T. Brumme, O. Bunau, M. Buongiorno Nardelli, M. Calandra, R. Car, C. Cavazzoni, D. Ceresoli, M. Cococcioni, N. Colonna, I. Carnimeo, A. Dal Corso, S. De Gironcoli, P. Delugas, R. A. DiStasio, A. Ferretti, A. Floris, G. Fratesi, G. Fugallo, R. Gebauer, U. Gerstmann, F. Giustino, T. Gorni, J. Jia, M. Kawamura, H.-Y. Ko, A. Kokalj, E. Küçükbenli, M. Lazzeri, M. Marsili, N. Marzari, F. Mauri, N. L. Nguyen, H.-V. Nguyen, A. Otero-de-la Roza, L. Paulatto, S. Poncé, D. Rocca, R. Sabatini, B. Santra, M. Schlipf, A. P. Seitsonen, A. Smogunov, I. Timrov, T. Thonhauser, P. Umari, N. Vast, X. Wu, and S. Baroni, Advanced capabilities for materials modelling with Quantum ESPRESSO, *J. Phys.: Condens. Matter* **29**, 465901 (2017).
- [50] A. Lughfi, Toward exact predictions of spin-phonon relaxation times: An ab initio implementation of open quantum systems theory, *Sci. Adv.* **8**, eabn7880 (2022).
- [51] J. G. C. Kragoskow, A. Mattioni, J. K. Staab, D. Reta, J. M. Skelton, and N. F. Chilton, Spin-phonon coupling and magnetic relaxation in single-molecule magnets, *Chem. Soc. Rev.* **52**, 4567 (2023).
- [52] E. Thingstad, A. Kamra, A. Brataas, and A. Sudbø, Chiral phonon transport induced by topological magnons, *Phys. Rev. Lett.* **122**, 107201 (2019).
- [53] T. Nomura, X.-X. Zhang, S. Zherlitsyn, J. Wosnitza, Y. Tokura, N. Nagaosa, and S. Seki, Phonon magnetochiral effect, *Phys. Rev. Lett.* **122**, 145901 (2019).
- [54] F. Wu, S. Bao, J. Zhou, Y. Wang, J. Sun, J. Wen, Y. Wan, and Q. Zhang, Fluctuation-enhanced phonon magnetic moments in a polar antiferromagnet, *Nat. Phys.* **19**, 1868 (2023).
- [55] S. Bao, Z.-L. Gu, Y. Shangguan, Z. Huang, J. Liao, X. Zhao, B. Zhang, Z.-Y. Dong, W. Wang, R. Kajimoto, M. Nakamura, T. Fennell, S.-L. Yu, J.-X. Li, and J. Wen, Direct observation of topological magnon polarons in a multiferroic material, *Nat. Commun.* **14**, 6093 (2023).
- [56] F. Wu, J. Zhou, S. Bao, L. Li, J. Wen, Y. Wan, and Q. Zhang, Magnetic switching of phonon angular momentum in a ferrimagnetic insulator, *Phys. Rev. Lett.* **134**, 236701 (2025).
- [57] Q. Wang, M.-Q. Long, and Y.-P. Wang, Magnetic moments of chiral phonons induced by coupling with magnons, *Phys. Rev. B* **110**, 024423 (2024).
- [58] H. Ning, T. Luo, B. Ilyas, E. V. Boström, J. Park, J. Kim, J.-G. Park, D. M. Juraschek, A. Rubio, and N. Gedik, Spontaneous emergence of phonon angular momentum through hybridization with magnons, [arXiv:2410.10693](https://arxiv.org/abs/2410.10693) (2024).
- [59] M. Weißenhofer, P. Rieger, M. S. Mrudul, L. Mikadze, U. Nowak, and P. M. Oppeneer, Chiral phonons arising from chirality-selective magnon-phonon coupling, *Phys. Rev. Lett.* **135**, 216701 (2025).
- [60] H. Bendin, A. Mook, I. Mertig, and R. R. Neumann, D-Wave Phonon Angular Momentum Texture in Altermagnets by Magnon-Phonon-Hybridization, [arXiv:2511.08357](https://arxiv.org/abs/2511.08357) [10.48550/arXiv.2511.08357](https://doi.org/10.48550/arXiv.2511.08357) (2025).
- [61] S. V. Gallego, J. M. Perez-Mato, L. Elcoro, E. S. Tasci, R. M. Hanson, K. Momma, M. I. Aroyo, and G. Madariaga, MAGNDATA: towards a database of magnetic structures. I. The commensurate case, *J. Appl. Crystallogr.* **49**, 1750 (2016).
- [62] S. V. Gallego, J. M. Perez-Mato, L. Elcoro, E. S. Tasci, R. M. Hanson, M. I. Aroyo, and G. Madariaga, MAGNDATA: towards a database of magnetic structures. II. The incommensurate case, *J. Appl. Crystallogr.* **49**, 1941 (2016).
- [63] A. Jain, S. P. Ong, G. Hautier, W. Chen, W. D. Richards, S. Dacek, S. Cholia, D. Gunter, D. Skinner, G. Ceder, and K. A. Persson, Commentary: The Materials Project: A materials genome approach to accelerating materials innovation, *APL Mater.* **1**, 011002 (2013).
- [64] Y. Liu, Y. Xu, S.-C. Zhang, and W. Duan, Model for topological phononics and phonon diode, *Phys. Rev. B* **96**, 064106 (2017).
- [65] P. Liu, J. Li, J. Han, X. Wan, and Q. Liu, Spin-group symmetry in magnetic materials with negligible spin-orbit coupling, *Phys. Rev. X* **12**, 021016 (2022).
- [66] X. Chen, J. Ren, Y. Zhu, Y. Yu, A. Zhang, P. Liu, J. Li, Y. Liu, C. Li, and Q. Liu, Enumeration and representation theory of spin space groups, *Phys. Rev. X* **14**, 031038 (2024).